Impact of Quantum Coherence on Inelastic Thermoelectric Devices: From Diode to Transistor

Bei Cao(曹蓓)[1], Chongze Han(韩崇泽)[1], Xiang Hao(郝翔)[1], Chen Wang(王晨)[2*], and Jincheng Lu(陆金成)[1*]

[1]*Jiangsu Key Laboratory of Micro and Nano Heat Fluid Flow Technology and Energy Application, School of Physical Science and Technology, Suzhou University of Science and Technology, Suzhou 215009, China*
[2]*Department of Physics, Zhejiang Normal University, Jinhua 321004, China*

(Received 6 March 2024; accepted manuscript online 19 June 2024)

We present a study on inelastic thermoelectric devices, wherein charge currents and electronic and phononic heat currents are intricately interconnected. The employment of double quantum dots in conjunction with a phonon reservoir positions them as promising candidates for quantum thermoelectric diodes and transistors. We illustrate that quantum coherence yields significant charge and Seebeck rectification effects. It is worth noting that, while the thermal transistor effect is observable in the linear response regime, especially when phonon-assisted inelastic processes dominate the transport, quantum coherence does not enhance thermal amplification. Our work may provide valuable insights for the optimization of inelastic thermoelectric devices.

DOI: 10.1088/0256-307X/41/7/077302

Phonon-based thermoelectricity has attracted significant research attention, owing to its relevance in both fundamental physics and cutting-edge energy applications.[1–3] Phonon-thermoelectric transport stands at the intersection of mesoscopic physics and opens quantum systems, exploring topics such as thermoelectric energy conversion in phonon-thermoelectric devices[4,5] and quantum dot (QD) circuit-quantum-electrodynamics.[6–8] Recently, various quantum phenomena based on QDs subjected to voltage bias and temperature gradients have been explored, revealing stressing the influence of quantum coherence on electron and phonon transport.[9–15] Coherence offers a promising viewpoint for investigating non-equilibrium open quantum systems, providing valuable insights for both theoretical foundations and practical applications.[16–21] However, exploration of phonon-thermoelectric devices with quantum coherence, e.g., diodes and transistors, is still on demand.

Inelastic thermoelectricity recently emerges as a rising front field, which opens up great potential for high-performance thermoelectric materials.[22–27] In a multiterminal setup, such as a three-terminal system, electronic and phononic heat currents are nonlinearly coupled due to inelastic electron–phonon interactions. These interactions involve at least three reservoirs, which is why we refer to the process as "inelastic transport." This term highlights the involvement of particles from different terminals, resulting in energy exchange facilitated by phonons. The control and separation of heat and electrical currents on mesoscopic scales have gained fundamental importance.[26,28–30] In particular, phonon-thermoelectric diode and transistor can be realized even in linear response regime, in the absence of negative differential thermal conductance.[31] In addition, inelastic thermoelectricity greatly broads the the working bound of quantum thermal devices.[32]

In this Letter, we delve into the realm of inelastic thermoelectric transport facilitated by phonons. We demonstrate that quantum coherence provides a promising avenue for realizing quantum thermoelectric devices. by employing the quantum master equation with full counting statistics approach, we showcase how the electron–phonon-interaction-induced nonlinearity allows for significant charge and Seebeck rectification effect by tuning the QD's energy levels. Furthermore, we illustrate that a three-terminal setup can exhibit thermal transistor effects even within the linear transport regime, whereas quantum coherence is detrimental to heat amplification effect. Our work establishes a robust platform offering unprecedented control over both charge and heat. Throughout this study, we set natural units $\hbar = k_{\rm B} = e \equiv 1$.

Model and Method. In our setup [see Fig. 1(a)], a double QD system is coupled to a phonon reservoir (ph), exchanging energy with two individual electronic reservoirs marked as L and R. The Hamiltonian reads[4]

$$\hat{H} = \hat{H}_{\rm DQD} + \hat{H}_{\rm e-ph} + \hat{H}_{\rm lead} + \hat{H}_{\rm tun} + \hat{H}_{\rm ph}. \quad (1)$$

Here, $\hat{H}_{\rm DQD} = \sum_{i={\rm l,\,r}} E_i \hat{d}_i^\dagger \hat{d}_i + t(\hat{d}_{\rm l}^\dagger \hat{d}_{\rm r} + {\rm H.c.})$ describes the QDs with their energies E_i, tunneling t, and electron creating (annihilating) operator $\hat{d}_i^\dagger(\hat{d}_i)$ in the i-th dot; $\hat{H}_{\rm e-ph} = \sum_q \lambda_q \hat{d}_{\rm l}^\dagger \hat{d}_{\rm r}(\hat{a}_q + \hat{a}_q^\dagger) + {\rm H.c.}$ accounts for electron–phonon interactions; $\hat{H}_{\rm ph} = \sum_q \omega_q \hat{a}_q^\dagger \hat{a}_q$ represents the phonon reservoir; $\hat{H}_{\rm lead} = \sum_{j={\rm L,\,R}} \sum_k E_{jk} \hat{d}_{jk}^\dagger \hat{d}_{jk}$ characterizes the electronic reservoirs' energy levels; $\hat{H}_{\rm tun} = \sum_k \gamma_{{\rm l},\,k} \hat{d}_{\rm l}^\dagger \hat{d}_{{\rm L},\,k} + \sum_k \gamma_{{\rm r},\,k} \hat{d}_{\rm r}^\dagger \hat{d}_{{\rm r},\,k} + {\rm H.c.}$ involves the tunnel-

*Corresponding authors. Email: wangchen@zjnu.cn; jinchenglu@usts.edu.cn
© 2024 Chinese Physical Society and IOP Publishing Ltd

ing between QDs and the reservoirs.

To analyze the thermoelectric device within the eigenbasis of the double QDs, we initiate the diagonalization of $\hat{H}_{\rm DQD}$ as follows:

$$\hat{H}_{\rm DQD} = E_{\rm D}\hat{D}^\dagger\hat{D} + E_{\rm d}\hat{d}^\dagger\hat{d}, \tag{2}$$

where $E_{\rm D} = \frac{E_{\rm r}+E_{\rm l}}{2} + \sqrt{\frac{(E_{\rm r}-E_{\rm l})^2}{4} + \Delta^2}$ and $E_{\rm d} = \frac{E_{\rm r}+E_{\rm l}}{2} - \sqrt{\frac{(E_{\rm r}-E_{\rm l})^2}{4} + \Delta^2}$ represent the eigenenergies, respectively. The new sets of Fermion operators are defined as $\hat{D} = \sin\theta\hat{d}_{\rm l} + \cos\theta\hat{d}_{\rm r}$ and $\hat{d} = \cos\theta\hat{d}_{\rm l} - \sin\theta\hat{d}_{\rm r}$,[33] with θ denoting $\arctan(\frac{2\Delta}{E_{\rm r}-E_{\rm l}})/2$. Consequently, the electron–phonon and dot–reservoir tunneling terms are reformulated as $\hat{H}_{\rm e-ph} = \sum_q \lambda_q[\sin(2\theta)(\hat{D}^\dagger\hat{D} - \hat{d}^\dagger\hat{d}) + \cos(2\theta)(d^\dagger D + D^\dagger d)](\hat{a}_q^\dagger + \hat{a}_q)$ and $\hat{H}_{\rm tun} = \sum_k[\gamma_{{\rm l},k}(\sin\theta\hat{D}^\dagger + \cos\theta\hat{d}^\dagger)\hat{d}_{{\rm L},k}, \gamma_{{\rm r},k}(\cos\theta\hat{D}^\dagger - \sin\theta\hat{d}^\dagger)\hat{d}_{{\rm r},k}] + {\rm H.c.}$ It can be inferred from the term $\hat{H}_{\rm e-ph}$ that within the eigenbasis of $\hat{H}_{\rm DQD}$, both dephasing and damping processes are included, which may cooperatively give rise to the steady-state coherence.

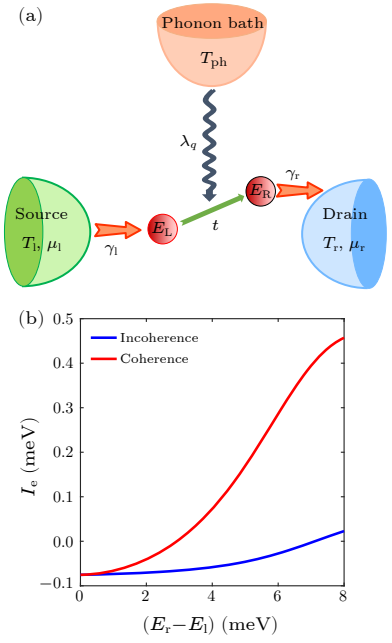

Fig. 1. (a) Illustration of the three-terminal inelastic thermoelectric device. An electron left the source into the left QD with energy $E_{\rm l}$ hopping to the right QD with a different energy $E_{\rm r}$ assisted by a phonon from the phonon reservoir (at temperature $T_{\rm ph}$). The temperatures and chemical potentials of two electric reservoirs are $T_{\rm L(R)}$ and $\mu_{\rm L(R)}$, respectively. The temperature of phonon reservoir is $T_{\rm ph}$; t is the tunneling between the two QDs, $\gamma_{\rm l}$ ($\gamma_{\rm r}$) is the coupling between the dots and the left (right) reservoir, and λ_q is the strength of electron–phonon interaction. (b) The charge current $I_{\rm e}$ as a function of level detuning $E_{\rm r} - E_{\rm l}$. The other parameters are taken as $\mu = 6\,{\rm meV}$, $\Delta\mu = 2\,{\rm meV}$, $E_{\rm l} = 0$, $\Gamma_{\rm l} = \Gamma_{\rm r} = \Gamma_{\rm ph} = 6\,{\rm meV}$, $t = 8\,{\rm meV}$, and $k_{\rm B}T_{\rm l} = k_{\rm B}T_{\rm r} = k_{\rm B}T_{\rm ph} = 10\,{\rm meV}$.

Based on the two-time measurement protocol,[34] we apply the full counting statistics to obtain the particle and energy flows out of electronic reservoirs and heat current out of phonon reservoir by including $\boldsymbol{\chi} = \{\lambda_p, \lambda_{\rm E}, \lambda_{\rm ph}\}$. Consequently, the counting-field-dependent total Hamiltonian is expressed as

$$H_{-\boldsymbol{\chi}/2} = H_{\rm DQD} + H_{\rm ph} + H_{\rm lead} + V_{-\boldsymbol{\chi}/2}, \tag{3}$$

with $V_{-\boldsymbol{\chi}/2}$ specified as

$$\begin{aligned} V_{-\boldsymbol{\chi}/2} = \sum_q \lambda_q[&\sin(2\theta)(\hat{D}^\dagger\hat{D} - \hat{d}^\dagger\hat{d}) \\ &+ \cos(2\theta)(d^\dagger D + D^\dagger d)]\left(e^{i\frac{\lambda_{\rm ph}}{2}\omega_q}\hat{a}_q + {\rm H.c.}\right) \\ &+ \sum_k([\gamma_{{\rm l},k}(\sin\theta\hat{D}^\dagger + \cos\theta\hat{d}^\dagger)\hat{d}_{{\rm L},k} \\ &+ \gamma_{{\rm r},k}e^{-i\frac{\lambda_p}{2}-i\frac{\lambda_{\rm E}}{2}E_{{\rm r},k}}(\cos\theta\hat{D}^\dagger - \sin\theta\hat{d}^\dagger)\hat{d}_{{\rm r},k}] \\ &+ {\rm H.c.}). \end{aligned} \tag{4}$$

We assume that the electron–phonon coupling and dot–reservoir tunnelings are weak. Based on the Born–Markov approximation, we perturb $V_{-\boldsymbol{\chi}/2}$ to obtain the quantum master equation as

$$\begin{aligned} \frac{\partial}{\partial t}\rho_{\rm S}(\boldsymbol{\chi}, t) &= i[\rho_{\rm S}(\boldsymbol{\chi}, t), H_{\rm DQD}] \\ &- \int_0^\infty d\tau {\rm Tr}_{\rm B}\{[[V_{-\boldsymbol{\chi}/2}, [V_{-\boldsymbol{\chi}/2}(-\tau), \rho_{\rm S}(\boldsymbol{\chi}, t)\otimes\rho_{\rm B}]_{\boldsymbol{\chi}}]_{\boldsymbol{\chi}}\}, \end{aligned} \tag{5}$$

where $\rho_{\rm S}(\boldsymbol{\chi}, t)$ denotes the reduced density operator of a central double-QD system with counting parameters, i.e., $\rho_{\rm S}(\boldsymbol{\chi}, t) = {\rm Tr}_{\rm B}\{\rho_{\boldsymbol{\chi}}^{\rm T}(t)\}$, with $\rho_{\boldsymbol{\chi}}^{\rm T}(t)$ being the full density operator of the whole inelastic thermoelectric device, the commutating relation denotes $[\hat{A}_{\boldsymbol{\chi}}, \hat{B}_{\boldsymbol{\chi}}]_{\boldsymbol{\chi}} = \hat{A}_{\boldsymbol{\chi}}\hat{B}_{\boldsymbol{\chi}} - \hat{B}_{\boldsymbol{\chi}}\hat{A}_{-\boldsymbol{\chi}}$, and the equilibrium distribution of reservoirs is specified as $\rho_{\rm B} = \rho_{\rm l}\otimes\rho_{\rm r}\otimes\rho_{\rm ph}$, with ρ_i being the density of matrix of the i-reservoir (i = L, R, ph). If we reorganize $\rho_{\rm S}(\boldsymbol{\chi}, t)$ in the vector form $|\boldsymbol{P}(\boldsymbol{\chi}, t)\rangle\rangle = [\langle 0|\rho_{\rm S}(\boldsymbol{\chi}, t)|0\rangle; \langle D|\rho_{\rm S}(\boldsymbol{\chi}, t)|D\rangle; \langle d|\rho_{\rm S}(\boldsymbol{\chi}, t)|d\rangle; \langle D|\rho_{\rm S}(\boldsymbol{\chi}, t)|d\rangle; \langle d|\rho_{\rm S}(\boldsymbol{\chi}, t)|D\rangle]$, the quantum master equation is reexpressed as

$$\frac{d|\boldsymbol{P}(\boldsymbol{\chi}, t)\rangle\rangle}{dt} = \boldsymbol{H}(\boldsymbol{\chi})|\boldsymbol{P}(\boldsymbol{\chi}, t)\rangle\rangle, \tag{6}$$

where $\boldsymbol{H}(\boldsymbol{\chi})$ is the evolution matrix. We note that the nonzero off-diagonal elements of the density matrix, i.e., $\langle D|\rho_{\rm S}(\boldsymbol{\chi}, t)|d\rangle$ and $\langle d|\rho_{\rm S}(\boldsymbol{\chi}, t)|D\rangle$, are the signature of quantum coherence. Conversely, if we want to neglect the quantum coherence effect, we consider the secular approximation to disregard the off-diagonal elements (see the Supplemental Material for details).

The charge, energy, and phonon currents flowing from the reservoir into the system are expressed, respectively, as

$$\begin{aligned} I_{\rm e}^{\rm r} &= \frac{\partial\mathcal{G}}{\partial(i\lambda_{\rm e})}|_{\chi=0}, \quad I_{\rm E}^{\rm r} = \frac{\partial\mathcal{G}}{\partial(i\lambda_{\rm E})}|_{\lambda=0}, \\ I_{\rm Q}^{\rm ph} &= \frac{\partial\mathcal{G}}{\partial(i\lambda_{\rm ph})}|_{\chi=0}, \end{aligned} \tag{7}$$

where $\mathcal{G} = \lim_{t\to\infty}\frac{1}{t}\ln\langle I|\boldsymbol{P}(\boldsymbol{\chi}, t)\rangle\rangle$ is the cumulant generating function, which can be alternatively taken as the minimal real part of the eigenvalues of the evolution matrix $\boldsymbol{H}(\chi)$.[35] The electronic heat current extracted from the right reservoir is defined as $I_{\rm Q}^{\rm r} = I_{\rm E}^{\rm r} - \mu_{\rm r}I_{\rm e}^{\rm r}$.[36] Similarly, the particle current $I_{\rm e}^{\rm l}$ and energy current $I_{\rm E}^{\rm l}$ flowing from the left (L) reservoir into the central system can also be

obtained by introducing the counting functions. Charge conservation implies that $I_{\rm e}^{\rm l}+I_{\rm e}^{\rm r}=0$, while the energy conservation requires $I_{\rm E}^{\rm l}+I_{\rm E}^{\rm r}+I_{\rm Q}^{\rm ph}=0$.[37]

Before delving into detailed discussions, it is essential to note that the methods employed in our study rely on weak system-reservoir couplings, denoted as γ_i ($i=$ l, r, ph). In a prior work,[38] we showcased the feasibility of periodically driven thermoelectric engines in a three-terminal double QDs system. Notably, we observed a substantial enhancement in both output work and efficiency due to the presence of quantum coherence. In Fig. 1(b), with a fixed chemical potential difference of $\Delta\mu=2\,{\rm meV}$, we present the net charge current $I_{\rm e}\equiv\frac{1}{2}(I_{\rm e}^{\rm r}-I_{\rm e}^{\rm l})$ as a function of the QD energy difference $E_{\rm r}-E_{\rm l}$ for both coherent and incoherent transports. It is evident that quantum coherence, characterized by nonzero off-diagonal elements in the system's density matrix, leads to a notable improvement in the charge current when compared to the scenarios in the absence of quantum coherence.

Diode Effect. Here we illustrate that the three-terminal configuration effectively behaves as the diode.[39–46] Our system, renowned for its combined thermal and electrical transport capabilities, offers the potential for unconventional rectification effect. Notably, it can induce charge rectification owing to a temperature difference, in addition to the conventional charge rectification driven by voltage bias.[31,33]

In a general nonequilibrium setup, the charge rectification effects can be characterized as

$$R_{\rm e}=\frac{|I_{\rm e}(\Delta\mu)+I_{\rm e}(-\Delta\mu)|}{|I_{\rm e}(\Delta\mu)|+|I_{\rm e}(-\Delta\mu)|},\tag{8}$$

which is induced by chemical potential. Such rectification induced by the temperature gradient, termed as Seebeck rectification, is expressed as[31]

$$R_{\rm et}=\frac{|I_{\rm e}(\Delta T)+I_{\rm e}(-\Delta T)|}{|I_{\rm e}(\Delta T)|+|I_{\rm e}(-\Delta T)|}.\tag{9}$$

Here, we demonstrate both charge and Seebeck-rectification effects in Fig. 2 based on the three-terminal QDs system. From Figs. 2(a) and 2(b), we find that the elastic heat and charge currents (i.e., $\Gamma_{\rm ph}=0$) are almost symmetrical, whereas the inelastic currents (i.e., $\Gamma_{\rm ph}\neq0$) become dramatic asymmetric. Hence, the microscopic inelastic electron–phonon scattering generally enhances the asymmetry of currents.[31]

Furthermore, we can make a comparative analysis between the charge rectification and Seebeck rectification effects in coherent and incoherent scenarios. Specifically, we study the influence of the QDs' energies $E_{\rm l}$ and $E_{\rm r}$ on rectification effects with and without quantum coherence. As depicted in Figs. 2(c)–2(e) and Figs. 2(d)–2(f), it becomes evident that both charge ($R_{\rm e}$) and Seebeck ($R_{\rm et}$) rectification effects in thermoelectric devices, when considering quantum coherence, are significantly more pronounced than the ones with incoherence. Hence, we can conclude that quantum coherence not only amplifies the current magnitudes but also intensifies the asymmetry of inelastic currents, thereby enhancing the rectification effects.

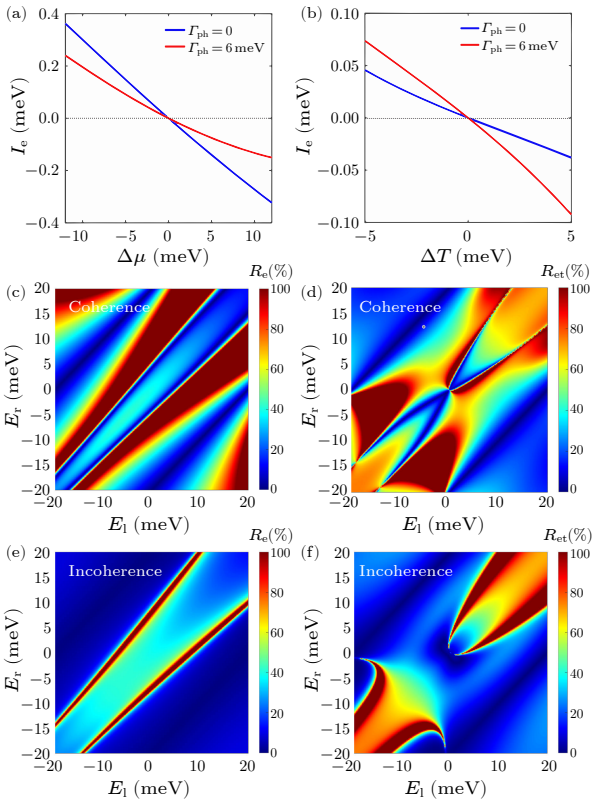

Fig. 2. Charge and Seebeck-rectification effects. (a) Charge current $I_{\rm e}$ as a function of $\Delta\mu$ for different $\Gamma_{\rm ph}$. The parameters are $\mu=0$, $E_{\rm l}=5\,{\rm meV}$, $E_{\rm r}=7\,{\rm meV}$, $k_{\rm B}T_{\rm ph}=10\,{\rm meV}$. (b) Charge current $I_{\rm e}$ as a function of ΔT for different $\Gamma_{\rm ph}$, where $\Delta\mu=0$, $E_{\rm l}=5\,{\rm meV}$, $E_{\rm r}=7\,{\rm meV}$. [(c), (e)] The charge rectification $R_{\rm e}$ as functions of QD energies $E_{\rm l}$ and $E_{\rm r}$ for (c) coherent transport and (e) incoherent transport, where $\Delta\mu=10\,{\rm meV}$ and $k_{\rm B}T_{\rm ph}=10\,{\rm meV}$. [(d), (f)] The Seebeck-rectification $R_{\rm et}$ as functions of QD energies $E_{\rm l}$ and $E_{\rm r}$ for (d) coherent transport and (f) incoherent transport, where $\Delta\mu=0$ and $k_{\rm B}T_{\rm ph}=15\,{\rm meV}$. The other parameters are given as $\Gamma_{\rm l}=\Gamma_{\rm r}=6\,{\rm meV}$, $t=8\,{\rm meV}$, $k_{\rm B}T_{\rm l}=k_{\rm B}T_{\rm r}=10\,{\rm meV}$.

Thermal Transistor Effect in the Linear-Response Regime. Heat amplification, a phenomenon that a minor adjustment in the base current yields a substantial impact on the current flowing between the collector and emitter, has led to the development of quantum thermal transistors, enabling precise control over energy transport.[47–49] As depicted in Fig. 3(a), this schematic outlines the operation of a conventional transistor. In our research, we investigate three-terminal quantum-dot systems as thermal transistors, as depicted in Fig. 3(b).

Traditionally, it was widely accepted that nonlinear transport is a prerequisite for thermal transistor effects. Negative differential thermal conductance was considered as a key condition for emergence of such effects, as outlined in Refs. [1,50,51]. However, a ground-breaking perspective was introduced in Ref. [31], proposing that thermal transistor effects could occur in the linear-transport regime, particularly when dominated by phonon-assisted inelastic transport. In our subsequent work,[7,33] we further demonstrated the existence of linear thermal transistor effects in circuit-quantum-electrodynamics systems across a wide

range of QD energies and light-matter interactions. Furthermore, we showed that thermal transistor effects can manifest even without these conditions in Brownian thermal transistors. Analyzing the statistical distributions of the thermal amplification factor within the Gaussian fluctuation framework provided further insights.[32] However, it is important to note that all these studies were limited to the quantum incoherent regime, and the influence of quantum coherence on the thermal transistor effect remains unexplored.

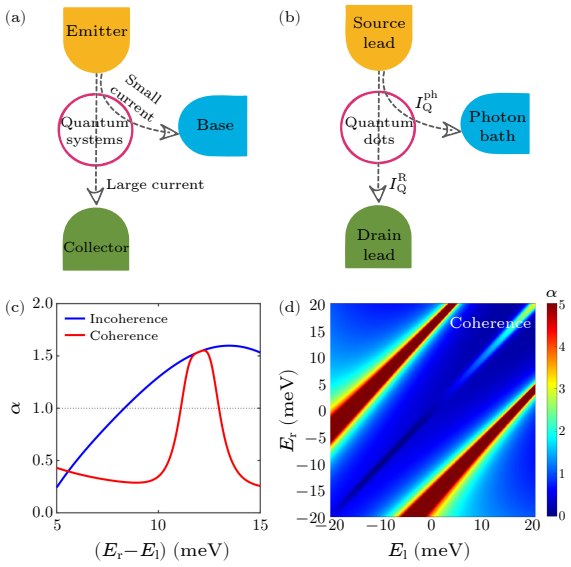

Fig. 3. (a) Schematic outlines the functioning of a conventional transistor. A small charge current originating from the emitter to the base governs a significantly larger charge current between the emitter and collector. The ratio between these two charge currents is the defining characteristic of the transistor effect. (b) Scheme of a three-terminal quantum-dot system that can serve as a phonon-thermoelectric transistor. Here, a modest heat current travels from the source lead to the phonon reservoir (I_Q^{ph}), and it exerts control over a substantial heat current flowing from the source lead to the drain lead (I_Q^r). This ratio between the two heat currents is known as the heat current amplification factor (α) and serves as the hallmark of the thermal transistor effect. (c) The heat current amplification factor α as a function of QD energy difference $E_l - E_r$ for the cases of coherence and incoherence. The other parameters are $\mu = 6\,\text{meV}$, $\Delta\mu = 0$, $E_l = 12\,\text{meV}$, $\Gamma_l = \Gamma_r = \Gamma_{ph} = 6\,\text{meV}$, $t = 8\,\text{meV}$, $k_B T_l = k_B T_r = k_B T_{ph} = 10\,\text{meV}$. (d) The heat current amplification factor α as functions of QD energy E_l and E_r. The other parameters are the same those in (c).

In the scenario of exclusively thermal conduction (with the electrochemical potential difference set to zero), the system's linear thermal transport properties can be aptly described by[52,53]

$$\begin{pmatrix} I_Q^r \\ I_Q^{ph} \end{pmatrix} = \begin{pmatrix} K_{RR} & K_{RP} \\ K_{PR} & K_{PP} \end{pmatrix} \begin{pmatrix} T_r - T_l \\ T_{ph} - T_l \end{pmatrix}. \tag{10}$$

One of our key findings is the potential for a thermal transistor effect to emerge within the linear-response regime. To be more specific, the amplification factor for heat current is defined as follows:

$$\alpha = \left| \frac{\partial_{T_{ph}} I_Q^r}{\partial_{T_{ph}} I_Q^{ph}} \right| = \frac{K_{RP}}{K_{PP}}. \tag{11}$$

As demonstrated in Figs. 3(c) and 3(d), we have observed that the coefficient α can be greater than 1 due to the inelastic transport process and displays high sensitivity to the quantum dot energies E_l and E_r, which can be easily manipulated through gate voltages in experimental setups. Initially, we observed that the thermal amplification effect could be achieved within a specific parameter range when $(E_r - E_l) > 8\,\text{meV}$ in the context of incoherent transport. However, when accounting for quantum coherence, while thermal amplification effects remain achievable, the range of $\alpha > 1$ becomes notably restricted specifically within $11\,\text{meV} < (E_r - E_l) < 13\,\text{meV}$. According to the findings in Ref. [31], the thermal amplification coefficient α is determined as $\alpha = |E_l/(E_r - E_l)|$ in the regime of weak electron–phonon coupling using the Fermi Golden rule method. The primary driver of the transistor effect is the ratio of incoherent thermal conductivity. Quantum coherence introduces interference effects, increases sensitivity to energy levels, and is susceptible to decoherence and noise, all of which narrow the parameter space for achieving the thermal transistor effect. Consequently, though quantum coherence significantly impacts currents as illustrated in Fig. 1(b), it does not facilitate the thermal transistor effect in the linear-transport regime, limiting rather than enhancing the conditions under which thermal amplification is possible. In summary, quantum coherence effects, though crucial for understanding the dynamics of quantum dot systems, restrict the thermal transistor effect in the linear response regime.

In conclusion, this study delves into the intriguing domain of inelastic thermoelectric devices, revealing their potential as quantum thermoelectric diodes and transistors via inelastic transport processes induced by electron–phonon interactions. We demonstrate that precise adjustment of QD energy levels can yield significant charge and Seebeck rectification effects, which are further enhanced when quantum coherence is considered. Additionally, our study has unveiled the capability of a three-terminal configuration to produce thermal transistor effects due to the inelastic transport, even within the linear transport regime. Nevertheless, it is important to note that quantum coherence does not contribute to heat amplification effect. In summary, our study underscores the significance of quantum coherence in the realm of inelastic thermoelectric devices and opens the door to innovative applications in the field of quantum thermoelectricity.

Acknowledgments. We thank Professor Jian-Hua Jiang, Professor Rafael Sánchez for helpful discussions. This work was supported by the National Natural Science Foundation of China (Grant No. 12305050), Jiangsu Key Disciplines of the Fourteenth Five-Year Plan (Grant No. 2021135), the Natural Science Foundation of Jiangsu Higher Education Institutions of China (Grant No. 23KJB140017), and the Opening Project of Shanghai

Key Laboratory of Special Artificial Microstructure Materials and Technology.

References

[1] Li N, Ren J, Wang L, Zhang G, Hänggi P, and Li B 2012 *Rev. Mod. Phys.* **84** 1045
[2] Thierschmann H, Sánchez R, Sothmann B, Arnold F, Heyn C, Hansen W, Buhmann H, and Molenkamp L W 2015 *Nat. Nanotech.* **10** 854
[3] Benenti G, Casati G, Saito K, and Whitney R S 2017 *Phys. Rep.* **694** 1
[4] Jiang J H, Entin-Wohlman O, and Imry Y 2012 *Phys. Rev. B* **85** 075412
[5] Jiang J H and Imry Y 2017 *Phys. Rev. Appl.* **7** 064001
[6] Liu H, Wang C, Wang L Q, and Ren J 2019 *Phys. Rev. E* **99** 032114
[7] Lu J, Wang R, Wang C, and Jiang J H 2023 *Entropy* **25** 498
[8] Ren J 2023 *Chin. Phys. Lett.* **40** 090501
[9] Bu K, Singh U, Fei S M, Pati A K, and Wu J 2017 *Phys. Rev. Lett.* **119** 150405
[10] Camati P A, Santos J F G, and Serra R M 2019 *Phys. Rev. A* **99** 062103
[11] Liu J and Segal D 2021 *Phys. Rev. E* **103** 032138
[12] Aimet S and Kwon H 2023 *Phys. Rev. A* **107** 012221
[13] Behera J, Bedkihal S, Agarwalla B K, and Bandyopadhyay M 2023 *Phys. Rev. B* **108** 165419
[14] Chen Z H, Wang F Y, Chen H, Lu J C, and Wang C 2023 *Chin. Phys. Lett.* **40** 050501
[15] Zhang C X, Li T J, Xu L J, and Huang J P 2023 *Chin. Phys. Lett.* **40** 054401
[16] Engel G S, Calhoun T R, Read E L, Ahn T K, Mančal T, Cheng Y C, Blankenship R E, and Fleming G R 2007 *Nature* **446** 782
[17] Alipasha V and Martin B P 2010 *New J. Phys.* **12** 085001
[18] Sánchez R, Gorini C, and Fleury G 2021 *Phys. Rev. B* **104** 115430
[19] Ivander F, Anto-Sztrikacs N, and Segal D 2022 *New J. Phys.* **24** 103010
[20] Yuan J H, Ruan H L, Liu D H, He J Z, and Wang J H 2023 *Chin. Phys. Lett.* **40** 100502
[21] Gao J Z, Liu X, Wang J H, and He J Z 2023 *Chin. Phys. Lett.* **40** 117301
[22] Wang R, Wang C, Lu J, and Jiang J H 2022 *Adv. Phys. X* **7** 2082317
[23] Entin-Wohlman O, Imry Y, and Aharony A 2010 *Phys. Rev. B* **82** 115314
[24] Lu J, Jiang J H, and Imry Y 2021 *Phys. Rev. B* **103** 085429
[25] Xi M, Wang R, Lu J, and Jiang J H 2021 *Chin. Phys. Lett.* **38** 088801
[26] Nian L L, Hu S Q, Xiong L, Lü J T, and Zheng B 2023 *Phys. Rev. B* **108** 085430
[27] Nian L L, Zheng B, and Lü J T 2023 *Phys. Rev. B* **107** L241405
[28] Pekola J P and Karimi B 2021 *Rev. Mod. Phys.* **93** 041001
[29] Lü J T, Wang J S, Hedegård P, and Brandbyge M 2016 *Phys. Rev. B* **93** 205404
[30] Li Y, Li W, Han T, Zheng X, Li J, Li B, Fan S, and Qiu C W 2021 *Nat. Rev. Mater.* **6** 488
[31] Jiang J H, Kulkarni M, Segal D, and Imry Y 2015 *Phys. Rev. B* **92** 045309
[32] Lu J, Wang R, Wang C, and Jiang J H 2020 *Phys. Rev. B* **102** 125405
[33] Lu J, Wang R, Ren J, Kulkarni M, and Jiang J H 2019 *Phys. Rev. B* **99** 035129
[34] Campisi M, Hänggi P, and Talkner P 2011 *Rev. Mod. Phys.* **83** 771
[35] Wang Z, Wang L Q, Chen J Z, Wang C, and Ren J 2022 *Front. Phys.* **17** 13201
[36] Yamamoto K and Hatano N 2015 *Phys. Rev. E* **92** 042165
[37] Jiang J H and Imry Y 2016 *C. R. Phys.* **17** 1047
[38] Lu J C, Wang Z, Ren J, Wang C, and Jiang J H 2024 *Phys. Rev. B* **109** 125407
[39] Zhang L, Wang J S, and Li B 2010 *Phys. Rev. B* **81** 100301
[40] Ren J and Zhu J X 2013 *Phys. Rev. B* **88** 094427
[41] Yang Y, Chen H, Wang H, Li N, and Zhang L 2018 *Phys. Rev. E* **98** 042131
[42] Zhang Y and Su S 2021 *Physica A* **584** 126347
[43] Wang C, Xu D, Liu H, and Gao X 2019 *Phys. Rev. E* **99** 042102
[44] Díaz I and Sánchez R 2021 *New J. Phys.* **23** 125006
[45] Tesser L, Bhandari B, Andrea Erdman P, Paladino E, Fazio R, and Taddei F 2022 *New J. Phys.* **24** 035001
[46] Khandelwal S, Perarnau-Llobet M, Seah S, Brunner N, and Haack G 2023 *Phys. Rev. Res.* **5** 013129
[47] Joulain K, Drevillon J, Ezzahri Y, and Ordonez-Miranda J 2016 *Phys. Rev. Lett.* **116** 200601
[48] Guo B Q, Liu T, and Yu C S 2018 *Phys. Rev. E* **98** 022118
[49] Yang Y, Zhao Y, and Zhang L 2023 *Appl. Phys. Lett.* **122** 232201
[50] Li B, Wang L, and Casati G 2004 *Phys. Rev. Lett.* **93** 184301
[51] Li B, Wang L, and Casati G 2006 *Appl. Phys. Lett.* **88** 143501
[52] Sánchez R, Thierschmann H, and Molenkamp L W 2017 *Phys. Rev. B* **95** 241401
[53] Wang C, Chen X M, Sun K W, and Ren J 2018 *Phys. Rev. A* **97** 052112